Relating fracture mechanics and fatigue lifetime prediction

Kalman Ziha University of Zagreb, Faculty of Mechanical Engineering and Naval Architecture
E-mail: kziha@fsb.hr Department of Naval Architecture and Ocean Engineering, Ivana Lucica 5, Zagreb, Croatia

Abstract: This article presents how to link together the results of fatigue crack growth tests, analytic fracture mechanics and experimental methods of fatigue lifetime predictions. The study at the beginning investigates the effect of mechanical load redistribution among failed and intact micro-structural bonds along fatigue crack growth to final crack at vulnerable locations in materials and structures under cyclic loads. The microstructural load redistribution model is analytically formulated as a mechanical interaction between fatigue crack growth and fatigue endurance on the macroscopic level. The article in continuation investigates how to link the parameters of fatigue crack growth in fracture mechanics to parameters of fatigue life directly from the work done on crack growth determined by testing. The article at the end illustrates the application of the analytic procedure for fatigue lifetime prediction that combines fracture mechanics and the load redistribution model for determination of S-N curve parameters important in structural analysis and design. In this research the fatigue life time parameters are derived from a single fatigue crack growth experiment instead from normally required sets of fatigue tests for different loading conditions.

Keywords: fatigue; fracture mechanics; crack growth; interaction; fatigue life; S-N curves;

1. Introduction

The aim of this work is to evaluate and verify fatigue characteristics of materials and structures under cyclic loads common to analytic fracture mechanics and experimental fatigue lifetime predictions straightforwardly from precisely recorded Fatigue Crack Growth (FCG) curves. The article keep hold of the characteristics of FCG and FCG rates as defined in fracture mechanics [1–3] by using Stress Intensity Factors (SIF) determined through investigation of stress fields in materials at the end of the crack [4-5]. Fatigue parameters in fracture mechanics in general can be determined analytically, by testing on carefully prepared test specimen [6–7] or computationally by using complex numerical models and finite element stress analysis [8-10]. The investigations in this article of practical analytical procedures in which fatigue parameters can be evaluated directly from FCG curves are encouraged through the reported improvements in precision of fatigue crack size measurements [11–12]. The article at the beginning presents the mechanical load redistribution model along the crack to its end on a lattice of microstructural particles in crystalline materials following the concept of crack growth kinetics [13]. The study reveals the empirical concept of Cause-and-Effect-Interaction (CEI) [14-17] for mathematical formulation of Fatigue crack growth and Endurance Interaction (FEI) induced by overstressing due to load redistribution under cyclic loads. The mechanical interaction model of load redistribution replaces in the article the commonly used numerical methods for fitting of crack growth and crack growth rate [18]. Lasting efforts and numerous experiments have been devoted since earlier [19] to investigation of fatigue life prediction methods [20] and of safer criteria for the prediction of fatigue failures [21].
It is recognized earlier in the energy-based approach how the local strain energy density can be taken as a consistent fatigue damage parameter [22- 26]. The strain energy-based life prediction criterion can be extended to include the effects of both mean stress and ratcheting [27]. Moreover, the Neuber's rule can be interpreted in terms of the total

energy densities [28]. It is also reported that the local strain energy approach to some types of welded joints showed a quite satisfactory assessment of the fatigue life [29]. A unified theory based on the cyclic strain energy density criterion can be applied for cumulative fatigue damage assessment [30]. The link between the strain energy density and the notch stress intensity factors is discussed recently considering some typical welded joints and sharp notches. The use of a coarse mesh in the finite element models and multiscaling based on local strain energy density evaluation were found promising [31-34] in fatigue analysis. The energy approach based on the internal strain energy density formulation has been found useful in practical computation of notch stress intensity factors [35]. The minimum strain energy density criterion can be modified by employing the von Mises elasto-plastic boundary [36]. Life prediction models have been developed with the energy-based approach to define a temperature-compensating parameter [37] as well as for thermo-mechanical fatigue [38] and for materials under biaxial loading [39]. It is also demonstrated that some processes in metallurgy such as martensite formation can be modeled as function of the cumulative strain energy density [40]. Investigation of temperature effects revealed that the plastic strain energy density was nearly invariant through the entire fatigue life [41].

However, in contrast to the energy formulation based on the internal strain energy density in materials under cyclic loads, the article investigates the possibility of extraction of fatigue life parameters directly from externally measurable work done along the crack growth obtainable by fatigue testing. The energy of resistance to cracking investigated in this article i.e. the energy absorption equivalent to the work done on crack growth by externally applied cyclic loads can be calculated through integration of experimentally derived FCG curves. The external energy approach based on work done on crack growth advocated in the article links the parameters of FCG to fracture mechanics for assessment of the fatigue life time parameters of S-N curves [42]. The mathematical FEI model elaborated in the article may provide additional analytical tool for faster evaluation and verification of fatigue life with less experimental efforts directly from a single FCG test.

Reported FCG test data for steel and weldments [43] were utilized in the article to demonstrate the application of the mathematical formulation developed in this research on the basis of load redistribution model and on FEI concept to support the analytical procedure for FCG presentation and fatigue life time prediction in materials engineering.

2. Mechanical load redistribution model of FCG

Fracture mechanics [1–3] focuses on changes of stress fields in materials under cyclic loads at the crack tip [4]. Instead, this aericle focuses on the possibility of interaction between the FCG and redistribution of loads among failed and intact micro-structural mechanical bonds of material particles along the growing crack to its end. The load redistribution process is described in the sequel on an example of a 2D square spring lattice [13] of bonds of equal or similar mechanical properties among material particles in a parallel systemic arrangement (Fig. 1). The stress $\sigma=F/N_f$ induced by uniaxial tensile cyclic force of fixed intensity in nominal amount of F activates successive bond failures at increasing failure rate in each load cycle N until the finite possible number N_f of bond failures in the vulnerable region (highlighted in Fig. 1a). After the first bond has failed, the load of unchanged intensity F redistributes in the second cycle to remaining N_f -1 bonds simultaneously increasing the stress in intact bonds to amount of $\sigma_1=F/(N_f-1)$. Subsequently, the load F redistributes after each of N cycles to remaining (N_f -N) intact bonds (for example, N_f=10 and for N=6 failed bonds see Fig. 1b). The result of the load redistribution after N cycles is that the remaining (N_f -N) intact

bonds are overloaded with stress in amount of $\sigma_N=F/(N_f-N)$ and consequently continue to fail at higher failure rate until all N_f bonds are broken. The load redistribution of remaining (N_f-N) bonds and the overstressing rate after N cycles (for example, for $N_f=10$, see left hand side in Table 1) are presented by the following term:

$$\frac{\sigma_N}{\sigma}=\frac{N_f}{N_f-N}=1+\frac{N}{N_f-N}=1+\frac{n_f}{1-n_f} \tag{2.1}$$

The overstressing rate $N/(N_f-N)$ in (2.1), where $n_f=N/N_f$ is the cyclic ratio, after N bond failures describes microstructural stress concentration on remaining intact bonds after load redistribution in amount of $N_f/(N_f-N)$. It also explains the interaction of the crack size after N cycles and the forthcoming crack growth on the macroscopic level with respect to the endurance of (N_f-N) remaining bonds. The accumulation of deteriorations of material mechanical properties and simultaneous reduction of endurance induced by continuous load redistribution and overstressing on micro-structural level on an interactive manner is perceptible as material yielding on macrostructural level.
The interaction FCG model based on the mechanical load redistribution under cyclic loads may be reminiscent to opening of a zip fastener and colloquially denoted as 'unzipping model' of FCG.

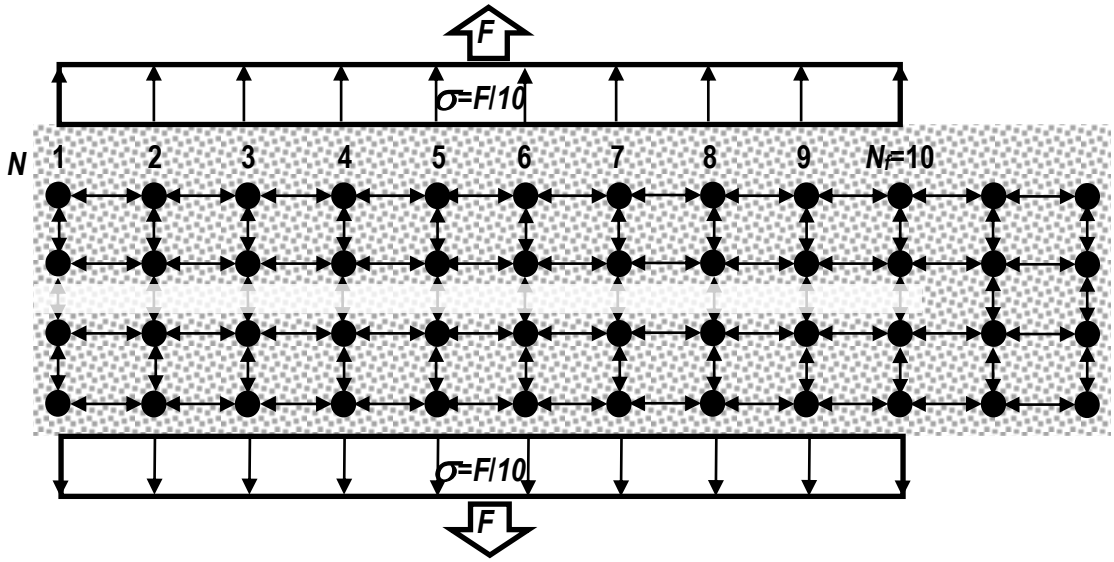

Figure 1a. Vulnerable region of $N_f=10$ bonds in a loaded 2D static square spring lattice model

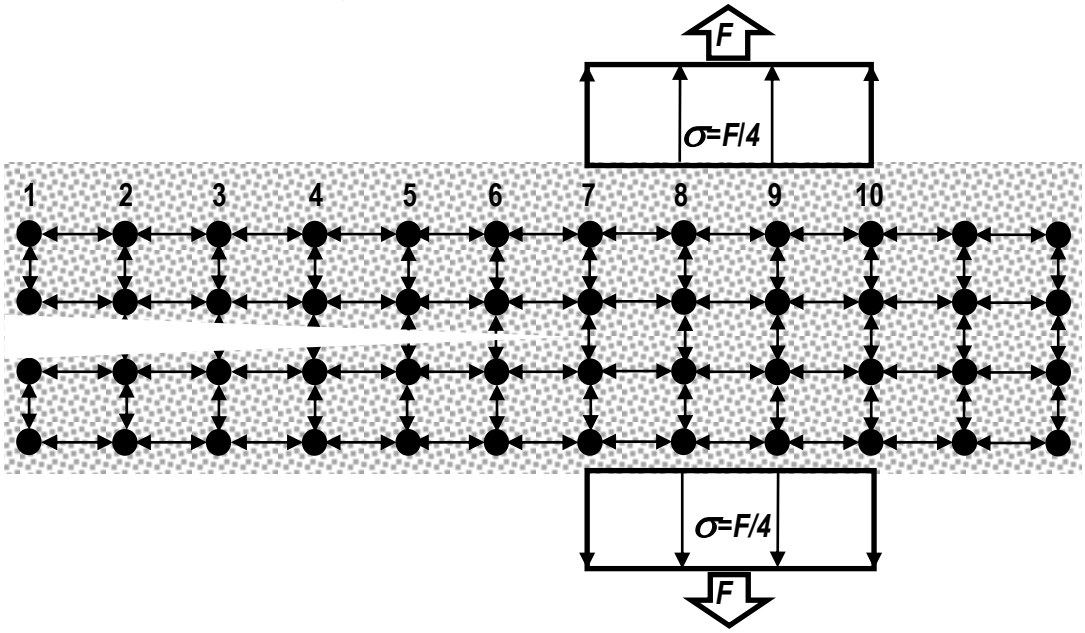

Figure 1b. Load redistribution from $N=6$ failed bonds to remaining 4 intact bonds

Table 1. Discrete load redistribution sequence and overstressing rate for N_f=10 bonds (Fig. 1)

N	N_f-N	n_f	*Redistribution* $N_f/(N_f-N)$	*Overstressing* $N/(N_f-N)$	$a_p(N)$	$a_i(N)$	$da(N)/dN$	$a(N)$ $a_p(N)+a_i(N)$	$U(N)$ $\int a(N)dN$
0	10	0	10/10=1+0/1	0.00	0	0.00	1+0.00	0.00	0,00
1	9	0.1	10/9=1+1/9	0.11	1	0.11	1+0.11	1.11	0,56
2	8	0.2	10/8=1+2/8	0.25	2	0.36	1+0.25	2.36	2,29
3	7	0.3	10/7=1+3/7	0.43	3	0.79	1+0.43	3.79	5,37
4	6	0.4	10/6=1+4/6	0.67	4	1.46	1+0.67	5.46	9,99
5	5	0.5	10/5=1+5/5	1.00	5	2.46	1+1.00	7.46	16,45
6	4	0.6	10/4=1+6/4	1.50	6	3.96	1+1.50	9.96	25,15
7	3	0.7	10/3=1+7/3	2.33	7	6.29	1+2.33	13.29	36,78
8	2	0.8	10/2=1+8/2	4.00	8	10.29	1+4.00	18.29	52,57
9	1	0.9	10/1=1+9/1	9.00	9	19.29	1+9.00	28.29	75,86
10	0	1.0	10/0=1+10/0	∞	10	∞	∞	∞	∞

3. Crack Growth – Endurance - Interaction model of FCG

In engineering of materials FCG is generally viewed as a Cause-and-Effect (CE) relation between progressing number N of cyclic loads (the cause C) and increasing crack size $a(N)$ (the effect E).

The hypothesis of the next study is that mechanical load redistribution and overstressing processes in which accumulation of degradation of material properties depends simultaneously on failure propagation and on residual strength can be described by the Cause-and-Effect-Interaction (CEI) concept [14–17]. Succinctly, the overstressing rate due to load redistribution after each subsequent load cycle N accelerates the forthcoming crack growth on expense of continuous diminution of finite fatigue endurance induced by the foregoing crack growth in interactive manner.

The primary crack size $a_p(n)$ starts to grow under each subsequent cyclic load of stress range $\Delta\sigma$ in some proportion p to the cyclic ratio n as shown:

$$a_p(n) = p \cdot n \tag{3.1}$$

The non-dimensional cyclic ratio $n=N/N_a$ represent the relative number of applied or observed load cycles with respect to the anticipated maximally possible number of load cycles N_a until observed final crack. In the same time, the endurance E has been reducing due to load redistribution after n load cycles in some possibly other proportion e to the remaining number of load cycles N_a-N or in terms of the cyclic ratio (1-n) (Fig. 2) as follows:

$$E(1-n) = e \cdot (1-n) \tag{3.2}$$

The rate of change of the secondary FCG $a_i(n)$ per cycle depends both on the progression of the primary FCG of size $a_p(n)$ (3.1) and on the drop of endurance $E(n)$ (3.2) (Fig. 3) due to mechanical overstressing of internal bonds in material induced by load redistribution (2.1) presented in the previous section and can be mathematically formulated as follows:

$$\frac{\mathrm{d}a_i(n)}{\mathrm{d}n} = \frac{p \cdot n}{e \cdot (1-n)} = i \cdot \frac{n}{1-n}. \tag{3.3}$$

The sensitivity $s(n)$ per cycle of FCG with respect to the number of cycles N is the derivative of (3.3) as shown:

$$s(n) = \mathrm{d}^2 a / \mathrm{d}n^2 = p + \frac{i}{(1-n)^2} \tag{3.4}$$

The sensitivity (3.4) indicates FCG acceleration due to decrease of endurance $(1-n)^2$ in final crack growth when $n \to 1$.

The example of discrete FCG and advancement of overstressing for N_f=10 bonds where $a_i(N)=N_a a_i(n)=\Sigma(N/(N_a-N)$ for N=1, 2, ..., 10, illustrates the mechanical load redistribution model. The work done on crack growth is then represented by the integral $U(N)=\int a(N)\mathrm{d}N$ (right hand side in Table 1).

The transition from micro to macro-structural level instead of the discrete model (2.1) (Table. 1, Fig.2 and Fig. 3) requires calculus for continuous analytic formulation of FCG for innumerable but finite number of bonds. The specific increase of the crack size in each load cycle of stress range $\Delta\sigma$, for example in *mm*/*cycles*, can be calculated as the integral up to an arbitrary number of cycles represented by the cyclic ratio n using (3.1-3.4) as follows:

$$a(n) = a_p(n) + a_i(n) = p \cdot n + \int_0^n \frac{\mathrm{d}a_i(n)}{\mathrm{d}n} dn = (p-i) \cdot n - i \cdot \ln(1-n) \tag{3.5}$$

The integration of (3.5) up to an arbitrary cyclic ratio n provides the expression for specific energy absorption of work done during crack growth per loading cycle that can be considered as the measure of fatigue strength equal to the energy of resistance to fatigue under cyclic stress of constant range $\Delta\sigma$, for example in *J*/(*N* x *cycles*) or in *mm*/*cycles*, as shown:

$$u(n) = \int_0^n a(n) dn = (p-i) \cdot n^2/2 + i \cdot \left[n + (1-n) \cdot \ln(1-n) \right] \tag{3.6}$$

For $n \to 1$ in (3.9) the full specific energy of resistance to cracking per cycle is $u(n)=(p+i)/2$ (Fig. 3).

The interaction intensity parameter i can be directly evaluated from the specific work u done on FCG (3.6) as follows:

$$i(n) = \frac{u(n) - p \cdot n^2/2}{\left[n - n^2/2 + (1-n) \cdot \ln(1-n) \right]} \tag{3.7}$$

The CEI model of FCG holds the load redistribution for the physical cause of interaction between the number of load cycles N of stress range $\Delta\sigma$ (the cause C) and the size of crack growth $a(N)$ (the effect E). The Fatigue crack growth and Endurance Interaction (3.3) denoted in the article as the FEI model describes the stress concentration process in remained intact parts along a crack in material caused by overstressing due to load redistribution during cyclic loading as described in previous section (2.1). The FEI is geometrically interpretable by continuous increase of the angle of tangent $n/(1-n)$ on the FCG curve during crack growth (Fig. 3). The crack size curve $a(N,\Delta\sigma)$ for anticipated asymptote N_a of crack growth under applied cyclic load of stress range $\Delta\sigma$, for example in *mm*, is then simply as shown:

$$a(N, \Delta\sigma) = N_a(\Delta\sigma) \cdot a(n) \tag{3.8}$$

The overall fatigue crack size $a(N)$ after N load cycles (3.8) consists of the primary linear growth $a_p(N)=N_a\, a_p(n)$ (3.1) that depends on the initial state of fatigue strength at the beginning of loading and of observable and quantifiable secondary growth $a_i(N)$ induced by the interaction between fatigue and endurance due to load redistribution. Propensity p expresses the initial state of fatigue strength of material or structure at the beginning of the loading process. The parameter $i=p/e$ in (3.3 - 3.6) is the measure of intensity of interaction of ensuing structural fatigue failures with the remaining fatigue endurance. The term (3.5) represents the fatigue yielding curve per cycle (Fig. 3) which characterizes the effect of overstressing and stress concentration due to load redistribution and the yielding induced by interaction between fatigue and endurance.

The next consideration aims to define and make practical use of the quantifiable work $W(N)$ done on crack growth until N cycles during fatigue testing under applied external cyclic load of constant stress range $\Delta\sigma_i$.

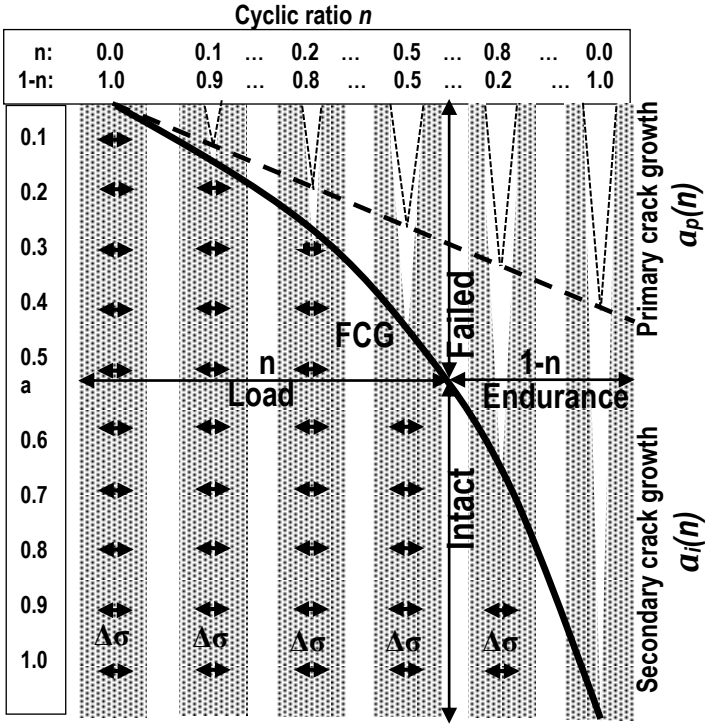

Figure 2. Load redistribution model of FCG

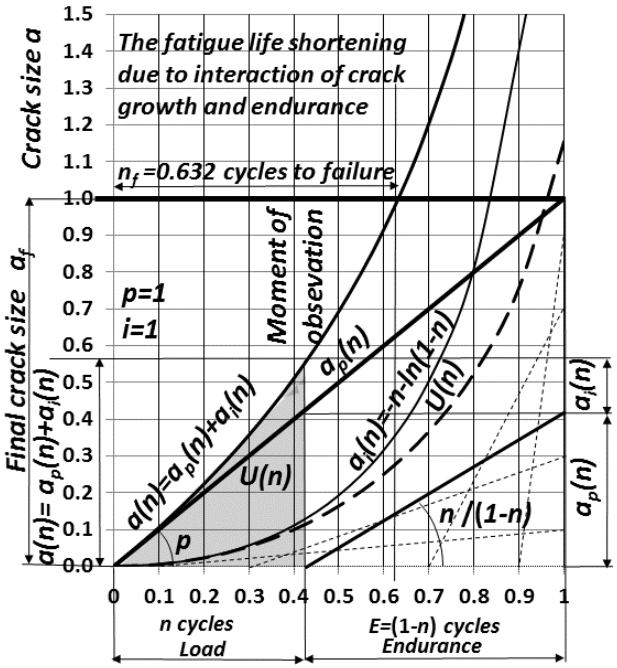

Figure 3. FEI between cyclic loads *n* and FCG *a*(*n*)

The area below the FCG curve (Fig. 3), for example in *mm* x *cycles*, may represent the work $W(N, \Delta\sigma)$ done on crack growth under cyclic test load of applied stress range $\Delta\sigma$ in ($\Delta\sigma$ x *a* x *N*)/$\Delta\sigma$, that can be calculated through numerical integration of experimentally derived FCG curves *a*(*N*). According to energy conservation principle, the work done on crack growth $W(N, \Delta\sigma)$ equals to the energy absorption $U(N, \Delta\sigma)$ that follows from the FEI model (3.7), for example in (*J* x *cycles*)/*N* or simply in *mm* x *cycles*, as shown:

$$U(N,\Delta\sigma) = N_a^2(\Delta\sigma)\cdot u(n) \qquad (3.9)$$

The mathematical formulation in the article explains the fatigue crack growth as an interrupted asymptotical logarithmic propagation till failure. The rapid increase of sensitivity towards the end of fatigue crack growth with respect to number of cyclic loads (3.4) in the asymptotic model strongly depends on the loss of fatigue endurance. This increase of sensitivity may explain the practically experienced high uncertainties of occurrences of fatigue failures induced by small material imperfections and environmental variability.

The analytic model presented in the article provides the important parameters of the FEI model in the fatigue analysis. The initial propensity to interaction represents the starting micro-structural constellation that can be derived from the state of fatigue strength of the material at the beginning of the test. The fatigue crack growth interaction intensity parameter expresses the effects of the average of massive successive progression of internal failures due to load redistribution and overstressing of the remaining intact bonds in material and can be calculated directly from the work done on the crack growth (3.8) derived from the experimentally recorded fatigue crack growth curves.

The computational procedure (3.1 to 3.9) may be supported by general non-linear optimization methods for determination and verification of essential parameters *p, i* and N_a of the FEI model..

4. Links among FCG test data, fracture mechanics and interaction model

FCG tests (t) under cyclic load of constant stress range $\Delta\sigma_t$ provide the crack sizes $a_t(N_t)$ for recorded numbers of load cycles N_t. Irwin's Stress Intensity Factor (SIF) range [4] at the end of a crack in Linear Elastic Fracture Mechanics (LEFM) can be calculated for the measured crack size a_t using the joint geometry function $Y(a_t)$ as a correction for crack growth limited by maximal crack size as shown:

$$\Delta K_t(a_t) = \Delta\sigma_t \cdot Y(a_t) \cdot \sqrt{\pi a_t} \tag{4.1}$$

The Paris-Erdogan's (PE) power rule [1-3] defines the crack growth rate during the steady FCG regime for $a_t(N_t)$ by slope m and the intercept C of the SIF range curve (4.1) fitted to straight line in double logarithmic scale, as follows:

$$\frac{\mathrm{d}a_t}{dN_t} = C \cdot \Delta K_t^{\,m}(a_t) \tag{4.2}$$

The steady FCG regime (4.2) commonly denoted in fracture mechanics as 'region two' starting after some number of cycles N_s at crack size a_s is commonly characterized by a threshold FCG rate, for example as $\mathrm{d}a/\mathrm{d}N=10^{-6}$ *mm*/*cycles*.

The governing hypothesis of the next study is that the FEI concept based on mechanical load redistribution model (3.1-3.9) is appropriate for the FCG analysis of experimental results for tested materials and structures. Consequently, the FCG curves defined by size a_t and number of cycles N_t following the FEI model (3.8) can replace other mathematical fitting methods such as secant or incremental polynomial methods [18] to smoothen N-a curves.

The study investigates in the sequel how the experimentally obtained FCG curves under test stress range $\Delta\sigma_t$ analytically described by FEI model (3.1-3.9) can be corrected to other stress ranges $\Delta\sigma$ (Fig. 4) using the definition of Irwin's SIF range (4.1) in fracture mechanics with sufficient accuracy comparing to integration of PE equation (4.2).

The record of fatigue test crack size curve a_t for some number of cycles N is employed for determination of the propensity p and the intensity i of the FEI model curve $a_t(N_t, \Delta\sigma_t)$ (3.8) in region two of FCG from cycles N_s to N_a as:

$$a_t(N, \Delta\sigma_t) = a_s + (N_a - N_s) \cdot a_t(n) = a_s + (N_a - N_s) \cdot \left[(p-i) \cdot n - i \cdot \ln(1-n) \right] \tag{4.3}$$

Note that in (4.3) a_s is the crack at $n=(N-N_s)/(N_a-N_s)=0$ at the start of continuous steady FCG regime from N_s to N_a.

By substituting the FCG rate $\mathrm{d}a_t/\mathrm{d}N$ that directly follows from the FCG curve a_t (4.3) into the PE equation (4.2) the parameters C and m in fracture mechanics are related to parameters p and i of the interaction FEI model as shown:

$$\frac{\mathrm{d}a_t}{\mathrm{d}N} = p + i \cdot \frac{n}{1-n} = C \cdot \Delta K_t^{\,m}(a_t) \tag{4.4}$$

The crack size a for arbitrarily selected stress range $\Delta\sigma$ can be related to the test crack size a_t for the applied test stress range $\Delta\sigma_t$ by employing the Irwin's SIF range values (4.1) at the test point (N_t, a_t) (Fig. 4) as shown:

$$a(N, \Delta\sigma) = a_t(N, \Delta\sigma_t) \cdot \left(\frac{\Delta\sigma_t}{\Delta\sigma} \right)^2 \cdot \left(\frac{Y(a_t)}{\Delta K(a_t)} \cdot \frac{\Delta K(a)}{Y(a)} \right)^2 \tag{4.5}$$

From the SIF range (4.1) and the PE equation (4.2) follows the FCG rate $\mathrm{d}a/\mathrm{d}N$ for stress range $\Delta\sigma$ as shown:

$$\frac{\mathrm{d}a}{\mathrm{d}N} = p + i \cdot \frac{n}{1-n} = \frac{da_t}{dN_t} \cdot \left(\frac{\Delta\sigma_t}{\Delta\sigma} \right)^{-m} \cdot \left(\frac{Y(a_t)}{Y(a)} \cdot \sqrt{\frac{a_t}{a}} \right)^{-m} \tag{4.6}$$

For crack sizes a equal to test values $a=a_t$, the number of cycles N with respect to values obtained by tests N_t in the steady crack growth regime (Fig. 4) is simply:

$$N = N_s + (N_t - N_s) \cdot \left(\frac{\Delta\sigma_t}{\Delta\sigma} \right)^m \tag{4.7}$$

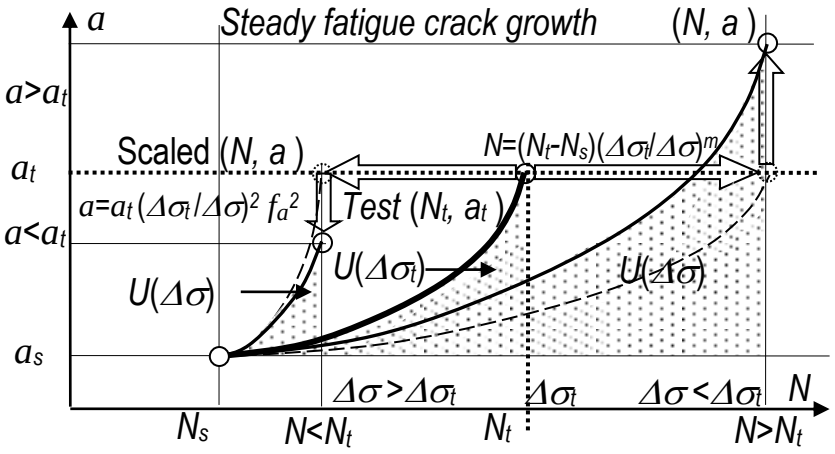

Figure 4. Scaling of experimental steady FCG curves in LFEM for different cyclic load ranges $\Delta\sigma$

5. Links between fracture mechanics and fatigue life

The stress-life (S-N) analytic procedure for fatigue life prediction in engineering of materials for steady FCG regime and high cycle low-strain response where the nominal strains are elastic is commonly based on Basquin's type equation [19] derived from the Hooke's law. This equation can be presented by standard S-N curves [22] in the simple form of a power rule as follows:

$$S^n \cdot N = A \tag{5.1}$$

In (5.1) S is the applied stress range $\Delta\sigma$ or often the stress amplitude $\Delta\sigma/2$, N is the number of cycles to failure or to transition from steady state to unsteady FCG regime, n is the inverse slope (Basquin constant) and A is the intercept of the S-N curve with the N axes, i.e. of a line in double logarithmic scale.

The hypothesis of the next study of fatigue life is that the specific energy absorption, that is the fatigue strength per load cycle $u(n,\Delta\sigma)=u_t(n_t,\Delta\sigma_t)$ (3.7) of a particular material or structure under calculational cyclic stress range $\Delta\sigma$ is equal to the specific energy absorption per load cycle u_t due to work done during steady FCG under applied test stress range $\Delta\sigma_t$.

The article investigates in the sequel the possibility for determination and verification of S-N curve parameters n and A in (5.1) directly from the specific energy absorption per cycle $u_t(n_t,\Delta\sigma_t)$ (3.7) of work done during steady FCG regime under test stress range $\Delta\sigma_t$. For this task in fatigue lifetime analysis are normally required sets of physical tests with a number of applied stress ranges $\Delta\sigma$ for fitting of the S-N curve shape based on Basquin's type of equation (5.1) to the shape of test data normally with some scatter requiring statistical analysis.

The energy $U(N,\Delta\sigma)$ absorbed at selected cyclic stress range $\Delta\sigma$ can be recalculated for crack size a equal to the recorded crack size $a=a_t$ (Fig. 4) using the energy $U(N_t,\Delta\sigma_t)$ equal to the work done $W(N_t,\Delta\sigma_t)$ during steady crack growth from N_s to N numbers of cycles (3.9) under testing stress range $\Delta\sigma_t$ following the principles of fracture mechanics (4.1-4.7) as shown:

$$U(N,\Delta\sigma)=\int_{N_s}^{N} a(N)dN=\left(\frac{\Delta\sigma_t}{\Delta\sigma}\right)^m\cdot\left(\frac{\Delta\sigma_t}{\Delta\sigma}\right)^2\cdot\int_{N_s}^{N_t}\left(\frac{Y(a_t)}{\Delta K(a_t)}\cdot\frac{\Delta K(a)}{Y(a)}\right)^2\cdot a_t(N,\Delta\sigma_t)dN \tag{5.2}$$

Scaling factor $f_a(\Delta\sigma)$ with respect to the known energy absorption determined in test condition under cyclic stress range $\Delta\sigma_t$ follows from (5.2) and for each applied stress range $\Delta\sigma$ can be calculated as shown:

$$\int_{N_s}^{N_t}\left(\frac{Y(a_t)}{\Delta K(a_t)}\cdot\frac{\Delta K(a)}{Y(a)}\right)^2\cdot a_t(N,\Delta\sigma_t)dN = f_a^2(\Delta\sigma)\cdot\int_{N_s}^{N_t} a_t(N,\Delta\sigma_t)dN = f_a^2(\Delta\sigma)\cdot U(N_t,\Delta\sigma_t) \tag{5.3}$$

The relation between the specific energy absorption under optional stress range $S=\Delta\sigma$ and under test stress range $S_t=\Delta\sigma_t$ follows from (5.3) and from the FEI model (3.9) in the following form:

$$\left(S^{\frac{m}{2}+1}\cdot(N-N_s)\right)^2\cdot u(n,\Delta\sigma)=\left(S_t^{\frac{m}{2}+1}\cdot f_a\cdot(N_t-N_s)\right)^2\cdot u_t(n_t,\Delta\sigma_t) \tag{5.4}$$

Accepting the hypothesis of constant fatigue strength $u=u_t$, the above relation (5.4) can be rewritten in the form of standard S-N curve format as $S^n N=A$ in (5.1) but additionally shifted with respect to total number of cycles N to transition from the steady to unsteady FCG.

The scaling factor $f_a(\Delta\sigma)$ in (5.3) represents the effects of crack size on crack growth for finite sheet implying the joint geometry function Y and the SIF range ΔK according to laws of fracture mechanics (4.5). For infinite sheet with constant joint geometry function $Y(a)$ and for critical SIF K_{cr} the correction factor is $f_a=1$. The value of the inverse slope n of S-N curve (Basquin's constant) in (5.1) for steady FCG regime in infinite sheet is then a simple linear function of the slope m of the SIF range curve according to PE law in (4.2) as presented below:

$$n=\frac{m}{2}+1 \tag{5.5}$$

For nonlinear or non-constant geometry function $Y(a)$ typical for finite sheets or structures and for critical SIF K_{cr} the scaling factor $f_a(\Delta\sigma)$ in (5.4) depends on the effect of crack size on crack growth $Y(a_t)/Y(a)$ for tested $\Delta\sigma_t$ and applied $\Delta\sigma$ stress ranges and can be adjusted by finding correction c to inverse slope n from the following condition:

$$\left(\frac{\Delta\sigma_t}{\Delta\sigma}\right)^{\frac{m}{2}+c}=\left(\frac{\Delta\sigma_t}{\Delta\sigma}\cdot f_a(\Delta\sigma)\right)^{\frac{m}{2}+1} \tag{5.6}$$

The correction c in (5.6) implies the changes caused by effect of crack size to crack growth for optional stress range $\Delta\sigma$ as shown:

$$c=1+\frac{\log\left[f_a(\Delta\sigma)\right]}{\log(\Delta\sigma_t/\Delta\sigma)} \tag{5.7}$$

The variable inverse slope n in (5.1) is modified for different stress ranges $\Delta\sigma$ for finite structures as follows:

$$n=\frac{m}{2}+c \tag{5.8}$$

The intercept A of the S-N curve with the N-axis in (5.1) follows from test data $\Delta\sigma_t$ *and* N_t. ,For appropriate value of FCG rate (4.2) that characterizes the transition from steady to unsteady FCG it is $A=\Delta\sigma_t^n N_t$ cycles. For the reported number of cycles to total fatigue failure of N_{ft} cycles under constant stress range $\Delta\sigma_t$, the S-N curve constant A with limited information about unsteady FCG, can be estimated for the same inverse slope n as $A=\Delta\sigma_t^n N_{ft}$ cycles.

The link between fracture mechanics and fatigue life (5.1-5.8) make possible to estimate the characteristics of S-N curves by numerical calculation for selected calculational values of stress ranges $\Delta\sigma$ instead of sets of tests with a number of material specimens under different cyclic loads.

6. Examples

In this section is demonstrated the appropriateness of the FEI model on examples of FCG tests reported for Base Material (BM) and for Friction Stir Welded joints (FSW) of AISI 409M grade ferritic stainless steel joints [43] (Figs. 5–10).

A. Firstly, the evaluation of interaction parameters of the FEI model based on the reported FCG curve for BM obtained under testing cyclic load of constant range $\Delta\sigma_t$=150 *MPa* at R=0.1 [43] is performed in following steps:

1. Numerical integration of reported data by using the trapezium rule provided the work done during steady FCG from size $2a_s$=6 *mm* at N_s=1620000 *cycles* to the crack size $2a_f$=16 *mm* after N_f=2670000 *cycles* in amount of $W(N_f)$=1700 *J x cycles*/*N*. The specific work, that is the fatigue strength per cycle is $u_t(n_f)= W(N_f)/(N_f-N_s)^2$=1.40*x*10^{-7} *J*/(*N x cycle*) (Figs. 5-7).
2. Propensity to interaction is assessed as the FCG rate p=d*a*/d*N*=2.17*x*10^{-6} *mm*/*cycle* at the start of steady FCG.
3. Intensity of interaction i=1.16*x*10^{-6} *mm*/*cycle* (3.8) is calculated directly from $u_t(n_f)$ (3.8) at the end of FCG.
4. Optimization program using evolutionary algorithm according to (3.1-3.9) provided the value of the asymptote at N_a=2720000 *cycles* that in combination with parameters p and i minimizes the FCG scatter. The scatter index SI=0.81% and the R-squared=0.9992 values indicate almost perfect fit between the crack size curve $a(N)$ defined by FEI model (4.3) and reported test values $a_t(N_t)$. Note that the scatter index SI is calculated as the root mean square error (RMSE) over mean of observations.

B. The computational procedure for determination of the SIF range values and PE power rule parameters based on the reported FCG curve for BM [43] for $\Delta\sigma_t$=150*MPa* provides following results:

1. The SIF range (4.1) is calculated using calculated FCG rate (3.3) (Fig. 7) and the geometry function $Y(a)=\sqrt{\frac{W}{\pi a}\cdot\tan\left|\frac{\pi a}{W}\right|}$ [43] for specimen width W=30 *mm* and crack size a defined (4.3) using the FEI procedure.
2. Best fit of SIF range in steady FCG regime (4.1-4.4) provides the slope m=4.66 and intercept C=2.58*x*10^{-10} (reported 4.66 and 2.58*x*10^{-10}) (Fig. 8).
3. For d*a*/d*N*=10^{-6} *mm*/*cycles* the threshold SIF range is ΔK_{th}=5.9 $MPa\sqrt{m}$ (reported 5.9). Reportedly, when the crack growth rate was around d*a*/d*N*=10^{-3} *mm*/*cycle* unstable crack growth occurred and the corresponding SIF range ΔK_{cr}=26 $MPa\sqrt{m}$ (reported 27) for transition from steady crack growth to unsteady-state was taken for critical SIF range [43] (Figs. 7 and 8).

C. The fatigue life parameters defining the S-N curve for BM (Figs. 9, 10) are found from the FCG test data obtained under constant stress range $\Delta\sigma_t$=150 *MPa* as follows:

1. For the calculated slope of the SIF range curve m=4.66, the inverse slope of the S-N curve without corrections for the effect of crack size on crack growth is calculated according to (5.10) as n=4.66/2+1=3.33.
2. The corrections f_a =(5.3), c (5.7), n (5.8) (Fig. 9) and appropriate numbers of cycles N_t for transition and N_{ft} for final failure (5.6) accounting for the effect of crack size on crack growth are obtained for calculational stress ranges $\Delta\sigma$ between 125 and 325 *MPa* (Table 2, Figs. 9).

3. The inverse slope of the S-N curve in amount of n=3.16 (reported n=3.14) that accounts for the corrections for the effect of crack size on crack growth is assessed for $\Delta\sigma_t$=150 *MPa* from Table 2 and Fig. 9.
   Note that the reported value n=3.14 is obtained by fitting to a set of fatigue life tests with four specimens for each of the five loading conditions [43].
4. The transition of steady to unsteady FCG for $\Delta\sigma_t$=150 *MPa* occurs reportedly at about FCG rate of da/dN=10^{-3} *mm*/*cycles* for calculated number of cycles N_t=2718700 calculated by FEI model (4.7) providing the S-N curve intercept A=2.26$x10^{+13}$ cycles (lower dashed line on Fig. 10).
5. For the reported number of cycles to total fatigue failure of N_{ft}=3600000 for $\Delta\sigma_t$=150 *MPa* the S-N curve constant is A_f=2.99$x10^{+13}$ cycles (upper full line on Fig. 10). Reportedly the stress range of $\Delta\sigma$=185 *MPa* corresponding to 2$x10^{+6}$ cycles was taken as an indication of the fatigue strength [43].

The scatter index for the reported S-N curve (n=3.14) with respect to reported experimental data is 37.11% (R-squared is 0.7416) and for calculated S-N curve data (n=3.16) is 37.58% (R-squared is 0.7349). The scatter index between the FEI calculated S-N curve data (n=3.16) and reported S-N curve (n=3.14) is 0.11% (R-squared is 0.9999) indicates very high matching of results.

Table 2. Corrections of S-N curves for the effect of crack size on crack growth for BM

$\Delta\sigma$	$\Delta\sigma_t/\Delta\sigma$	N *test*	f_a (5.3)	c (5.7)	n (5.8)	Nt *Transition*	Nft *Failure*
125	1.20	4500000	0.958	0.77	3.10	4854647	642834
150	1.00	3600000	1.000	0.84	3.16	2718642	359992
175	0.86	2700000	1.020	0.87	3.20	1665216	220501
225	0.67	1120000	1.037	0.91	3.24	748844	991590
275	0.55	640000	1.045	0.93	3.26	395597	523835
325	0.46	300000	1.048	0.94	3.27	232564	307952

D. Secondly, the evaluation of interaction parameters of the FEI model based on the reported FCG curve for FSW obtained under testing cyclic load of constant range $\Delta\sigma_t$=150 *MPa* at R=0.1 [43] is performed in following steps:

1. Numerical integration of reported data by using the trapezium rule provided the work done during steady FCG from size 2a_s=6 *mm* at N_s=2500000 *cycles* to crack size 2a_f=16 *mm* after N_f=4180000 *cycles* in amount of $W(N_f)$=2200 *J x cycles*/*N*. The specific work, that is the fatigue strength per cycle is then $u_t(n_f)= W(N_f)/(N_f-N_s)^2$=7.44$x10^{-7}$ *J*/(*N x cycle*) (Figs. 5-7).
2. Propensity to interaction is assessed as the FCG rate p=da/dN=9.47$x10^{-6}$ *mm*/*cycle* at the start of steady FCG.
3. Intensity of interaction i=7.02$x10^{-7}$ *mm*/*cycle* (3.8) is calculated directly from $u_t(n_f)$ (3.8) to the end of FCG.
4. Optimization program using evolutionary algorithm according to (3.1-3.9) provided the value of the asymptote at N_a=4220000 *cycles* that in combination with parameters p and i minimizes the FCG scatter. The scatter index SI=1.02% and the R-squared=0.9985 indicate very high fit between the crack size curve $a(N)$ defined by FEI model (4.3) and reported test values $a_t(N_t)$.

E. The computational procedure for determination of the SIF range values and PE power rule parameters based on the reported FCG curve for FSW [43] for $\Delta\sigma_t$=150*MPa* provides following results:

1. The SIF range (4.1) is calculated using calculated FCG rate (3.3) (Fig. 7) and the geometry function $Y(a)=\sqrt{\frac{W}{\pi a}\cdot\tan\left|\frac{\pi a}{W}\right|}$ [43] for specimen width W=30 *mm* and crack size a defined (4.3) using the FEI procedure.

2. Best fit of SIF range in steady FCG regime (4.1-4.4) provides the slope m=3.78 and intercept C=3.20x10^{-10} (reported 3.78 and 7.48x10^{-10}) (Fig. 8).
3. For da/dN=10^{-6} *mm*/*cycles* the threshold SIF range is ΔK_{th}=8.4 $MPa\sqrt{m}$ (reported 8.2). Reportedly, when the crack growth rate was around da/dN=10^{-3} *mm*/*cycle* unstable crack growth occurred and the corresponding SIF range ΔK_{cr}=53 $MPa\sqrt{m}$ (reported 55) for transition from steady crack growth to unsteady-state was taken for critical SIF range [43] (Figs. 7 and 8).

F. The fatigue life parameters defining the S-N curve for FSW (Figs. 9, 10) are found from the FCG test data obtained under constant stress range $\Delta\sigma_t$=150 *MPa* as follows:

1. For the calculated slope of the SIF range curve m=3.78, the inverse slope of the S-N curve without corrections for the effect of crack size on crack growth is calculated according to (5.10) as n=3.78/2+1=2.89.
2. The inverse slope of the S-N curve in amount of n=2.75 (reported n=2.44) that accounts for the corrections for the effect of crack size on crack growth is assessed for $\Delta\sigma_t$=150 *MPa* from Table 3 and Fig. 9.
3. The transition of steady to unsteady FCG for $\Delta\sigma_t$=150 *MPa* occurs reportedly at about FCG rate of da/dN=10^{-3} *mm*/*cycles* for number of cycles N_t=4218800 calculated by FEI model (4.7) providing the S-N curve intercept A=4.07x10^{+12} cycles (lower dashed line on Fig. 10).
4. For the reported number of cycles to total fatigue failure of N_{ft}=3600000 for $\Delta\sigma_t$=150 *MPa* the S-N curve constant is A_f=5.01x10^{+12} cycles (upper full line on Fig. 10). Reportedly the stress range of $\Delta\sigma$=230 *MPa* corresponding to 2x10^{+6} cycles was taken as an indication of the fatigue strength [43]. The scatter index (SI=RMSE/MV) for the reported S-N curve (n=2.44) with respect to reported experimental data is 15.00% (R-squared is 0.9757) and for calculated S-N curve data (n=2.75) is 21.50% (R-squared is 0.9502). The scatter index between the FEI calculated S-N curve data (n=2.75) and reported S-N curve (n=2.44) is 7.40% (R-squared is 0.9945) indicates slightly lower but still good matching of results.

Table 3. Corrections of S-N curves for the effect of crack size on crack growth for FSW

$\Delta\sigma$	$\Delta\sigma_t/\Delta\sigma$	N *test*	f_a (5.3)	c (5.7)	n (5.8)	Nt *Transition*	Nft *Failure*
125	1.20	4500000	0.958	0.77	2.70	6965204	858522
150	1.00	3600000	1.000	0.84	2.75	4217993	519904
175	0.86	2700000	1.020	0.87	2.78	2761098	340329
225	0.67	1120000	1.037	0.91	2.81	1383358	170511
275	0.55	640000	1.045	0.93	2.83	796657	981950
325	0.46	300000	1.048	0.94	2.84	503219	620262

Note: The results in examples are derived in MS-Excel work sheets using intrinsic Solver add-ins with evolutionary algorithm and Generalized Reduced Gradient (GRG) optimization methods.

7. Discussion

Examples in this article confirmed the agreement of calculated and reported data. However, the differences can be understood having on mind that the methods of fracture mechanics applied in this research for fatigue lifetime assessments are developed for steady FCG regime known as ‘region two’, since the experimental methods consider the whole span of lifetime with high statistical scatter of test data till total failure including the unstable FCG known as ‘region three’.

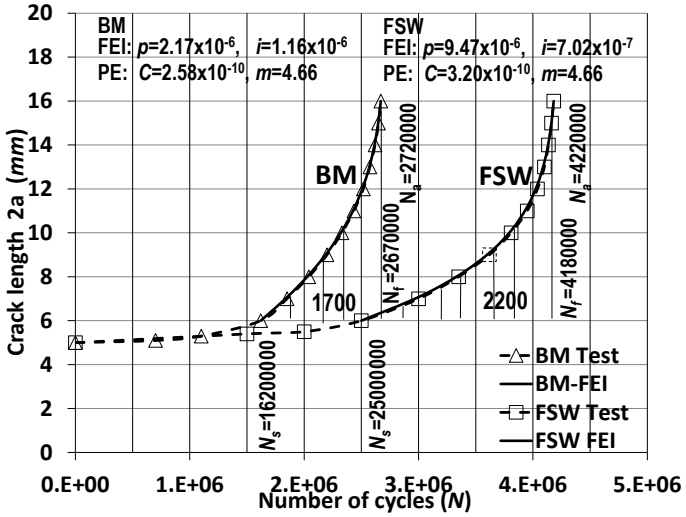

Figure 5. FCG sizes $a(N)$ for BM and FSW

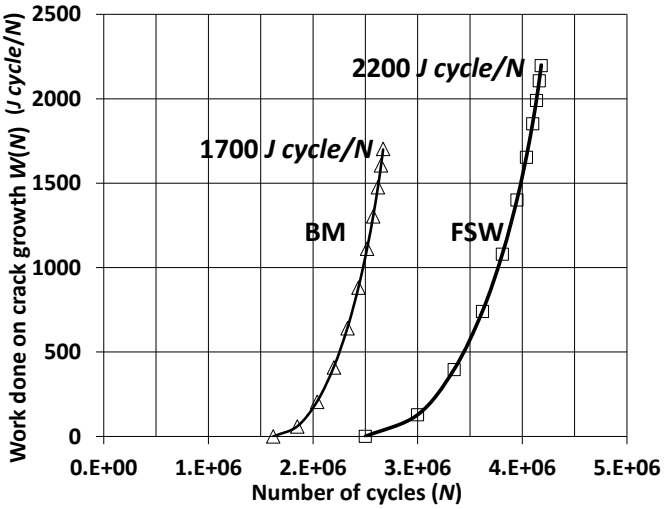

Figure 6. Energy absorption due to work done on FCG

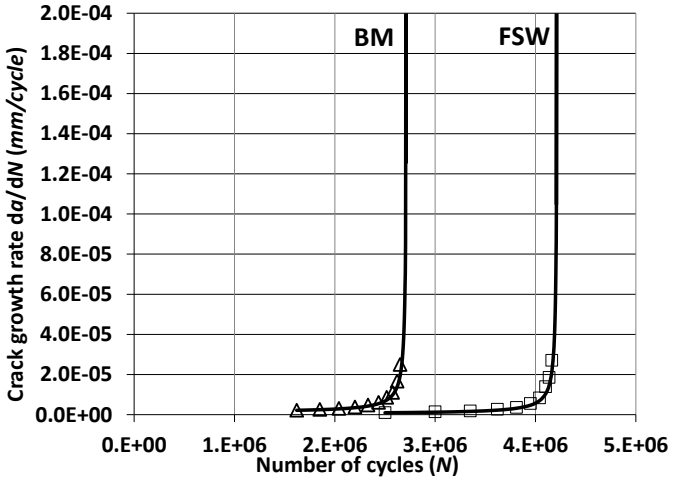

Figure 7. FCG rates d$a(N)$/dN for BM and FSW

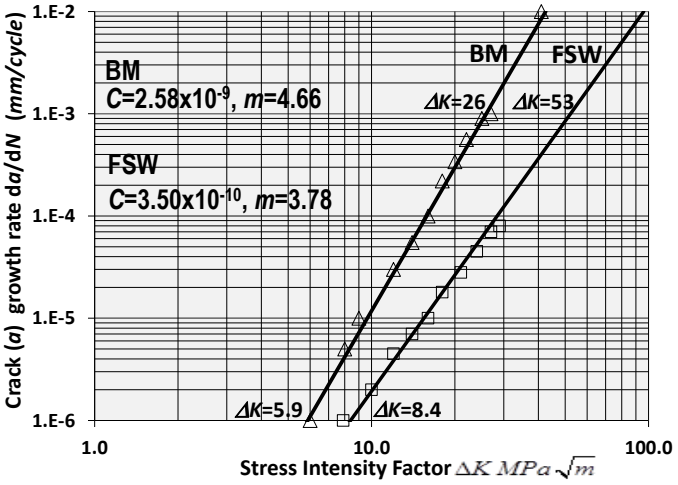

Figure 8. Stress intensity factor ranges ΔK(da/dN)

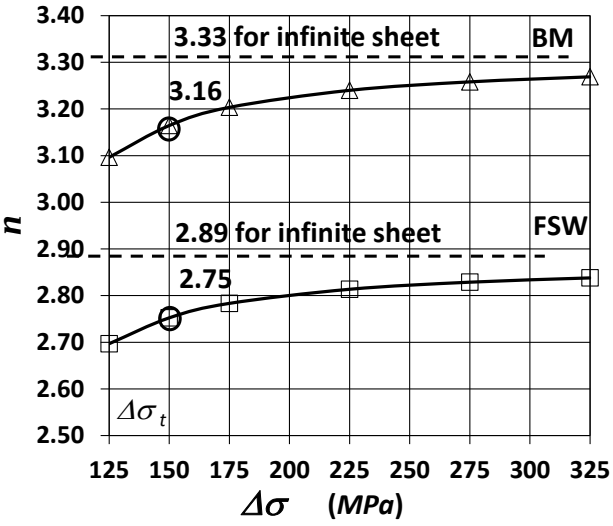

Figure 9. Inverse slopes n of S-N curves for BM and FSW

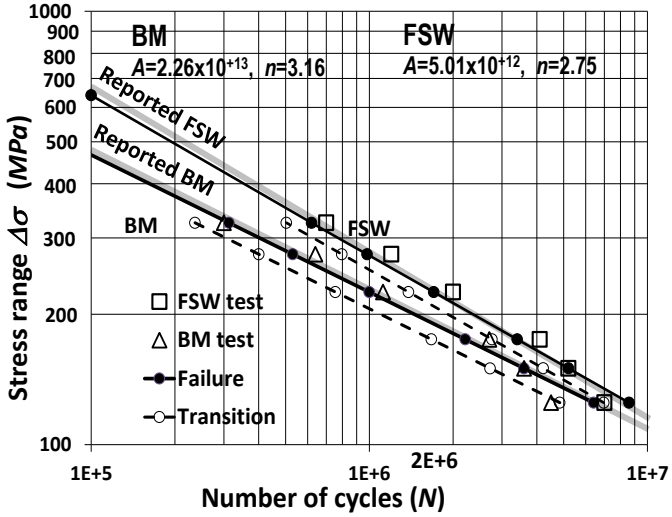

Figure 10. S-N curves for BM and FSW

Conclusion

The article elaborates the link between analytic fracture mechanics, fatigue crack growth tests and experimental lifetime predictions in materials science and engineering.

The results of calculations performed on the reported fatigue test data uphold the thesis revealed at the beginning of the article that the macroscopically observable fatigue crack growth can be modeled as a mechanical yielding process induced by overstressing due to redistribution of loads among huge but finite number of failed and intact internal micro-structural bonds. Interpretation of fatigue experiments in this study allows rethinking of the argument that there are measurable interactions between the preceding fatigue crack growth and impending fatigue endurance. Consequently, fatigue crack growth is regarded in the study as an interaction governed by propensity to and intensity of interaction between the increasing number of load cycles and the resulting crack growth that simultaneously affects and is affected by the residual fatigue endurance. The fatigue crack growth-endurance-interaction model in the article replaces the numerical fitting methods for analytic definition of experimental fatigue crack growth and fatigue crack growth rate for definition of stress intensity factors suitable for steady fatigue crack growth in fracture mechanics. The interaction model provides the mathematical formulation of energy conservation principle between the work done on crack growth under external cyclic loadings and the energy absorption due to internal material resistance to fatigue propagation all over the fatigue life that can be considered as the measure of fatigue strength.

The research of fatigue lifetime in continuation of this article corroborates the thesis that the fatigue life parameters can be extracted directly from a single experimentally derived FCG curve. The internal energy of resistance to cracking i.e. the energy absorption equivalent to the work done by cyclic external forces on crack growth can be calculated through numerical integration of precisely recorded crack size. Accordingly, the article reinterprets the Basquin's equation for prediction of fatigue life as the relation of the energy absorption of work done during fatigue crack growth for different applied cyclic loads until fatigue failure of test specimens or of realistic structures. The method presented in the article allows assessment of the parameters of S-N curves of importance to life time predictions directly from a single fatigue crack growth experiment rather than from sets of stress-life tests of lifetime duration to failure under various loading conditions. The article recommended analytical corrections for the effect of crack size on crack growth for finite geometries of specimens and structures in order to provide S-N curves for practical use in their standardized form. The number of repeated physical FCG test to failure can be replaced by a numerical procedure for different loading conditions illustrated by examples in the article. The method exposed in this article is found sufficiently simple and numerically accurate for application to problems of fatigue in engineering of materials appropriate for structural analysis and design.

Acknowledgement

This work was supported by the Ministry of Science, Education and Sports of the Republic of Croatia under grant No. 120-1201703-1702.

Nomenclature

a	crack size
A	intercept of S-N curves
c	correction of S-N curve slope for crack size
C	intercept of SIF range curves
CE	Cause-Effect relation
CEI	Cause-Effect-Interaction
E	fatigue endurance
f_a	scaling factor for effects of crack size
FCG	Fatigue Crack Growth
FEI	Fatigue-Endurance-Interaction
i	interaction intensity FEI parameter
m	slope of SIF range curves
n	inverse slope of S-N curves, also cyclic ratio
N	number of loading cycles
p	propensity to interaction FEI parameter
PE	Paris-Erdogan power rule
R	stress ratio
s	sensitivity to cracking
S	stress range $\Delta\sigma$ or amplitude in S-N approach
SI	scatter index
SIF	stress intensity factor
Y	joint geometric function
W	specimen width
ΔK	stress intensity factor (SIF) range
$\Delta\sigma$	cyclic stress range

References

[1] P. Paris, F. Erdogan, A critical analysis of crack propagation laws. Journal of Basic Engineering, Trans. ASME, 528-534, 1963.

[2] N. Pugno, M. Ciavarella, P. Conneti, A. Carpinteri, A generalized Paris' low for fatigue crack growth. Journal of the Mechanics and Physics of Solids, **54** 1333-1349, 2006.

[3] B. Brighenti, A. Carpinteri, N. Corbari, Damage mechanics and Paris regime in fatigue life assessment of metals. International Journal of Pressure Vessels and Piping, **104** 57-68, 2013.

[4] G.R. Irwin, Analysis of stress and strains near the end of a crack traversing a plate. Journal of Applied Mechanics **24** 3 361–364, 1957.

[5] C. Macabe, H. Kaneshiro, S. Nishida, H. Sakihama, A Consideration on Evaluation of Fatigue-Crack Propagation Rate from Effective Stress Intensity Factor Range. Journal of Testing and Evaluation, **23** 3 153-159, 1995.

[6] P. Ljustell, F. Nilssen, Effects of different load schemes on the fatigue crack growth rate. Journal of Testing and Evaluation, **34** 4 333-441, 2006.

[7] E.R. Abril, The influence of initial crack length on critical stress intensity factor K-1. Journal of Testing and Evaluation, **34** 3 430-436, 2006.

[8] D. Benuzzi, E. Bormetti, G. Donzella, Stress intensity factor range and propagation mode of surface cracks under rolling-sliding contact. Theoretical and Applied Fracture Mechanics, **40** 1 55-74, 2003**.**

[9] X.P. Huang, T. Moan, W.C. Cui, An engineering model of fatigue crack growth under variable amplitude loading. International Journal of Fatigue, **30** 1 2-10, 2007.

[10] A. Carpinteri, R. Brighenti, S. Vantadori, Influence of the cold-drawing process on fatigue crack growth of a V-notched round bar. International Journal of Fatigue, **32** 7 1136-1145, 2010.

[11] M. Oore, Minimization and Quantification of Error Associated With the K-Gradient and the Interval of Crack Length Measurement in Fatigue Crack-Growth Testing. Journal of Testing and Evaluation, **21** 2 107-113, 1993.

[12] H.Y., Chung, S.H., Liu, R.S. Lin, S.H. Ju, Assessment of stress intensity factors for load-carrying fillet welded cruciform joints using a digital camera. International Journal of Fatigue, **30** 10-11 1861–1872, 2008.

[13] I. L. Slepian, Models and Phenomena in Fracture Mechanics, Springer 2002

[14] K. Ziha, Fatigue Yield. International Journal of Fatigue, **31** 7 1211–1214, 2009.

[15] K. Ziha, Stress-Strain Interaction Model of Plasticity. Acta Polytechnica Hungarica, **12** 1 42-54, 2015.

[16] K. Ziha, Modeling of worsening. Journal of Systemics, Cybernetics and Informatics, **10** 4 11-16, 2012.

[17] K. Ziha, Cause-and-Effect Interactions in Natural Sciences, Journal of Pensee, **76** 3 Part 3, 2014.

[18] ASTM E647-08 Standard Test Method for Measurements of Fatigue Crack Growth Rates. ASTM Intern., 2005.

[19] O. H. Basquin, The exponential law of endurance tests, Proc. ASTM, **10** 625–630, 1910.

[20] S. Stefanov, Fatigue Life Prediction without Cycle Counting (by Means of the Integral Method). Journal of Theoretical and Applied Mechanics, **32** 1 34-47, 2002**.**

[21] E. Macha, C.M. Sonsino, Energy criteria of multiaxial fatigue failure. Fatigue and Fracture of Engineering Materials and Structures. **22** 1053-1070, 1999.

[22] D. Kujawski, Fatigue Faulure Crierion Based on Strain Energy Density, Mechanika Teoretyczna i Stosowana, **1** 27, 1989.

[23] D. Kujawski, F. Ellyn, A fatigue crack propagation model, Engineering Fracture Mechanics **20** 5-20 695-707, 1984.

[24] D. Kujawski, F. Ellyn, A cumulative damage theory for fatigue crack initiation and propagation, International Journal of Fatigue **6** 2-6 83-88, 1984.

[25] F. Ellyn, D. Kujawski, Plastic Strain Energy in Fatigue Failure, Journal of Pressure Vessel Technology 11/1984; 106(4). DOI:10.1115/1.3264362 · 0.36 Impact Factor

[26] Kujawski, F. Ellyn, A unified approach to mean stress effect on fatigue threshold conditions, International Journal of Fatigue **17** 2 101-106, 1995.

[27] Z. Xia, Kujawski, F. Ellyn, Effect of mean stress and ratcheting strain on fatigue life of materials, International Journal of Fatigue **18** 5 335-341, 1996.

[28] D. Kujawski, On energy interpretations of the Neuber's rule, Theoretical and Applied Fracture Mechanics **73** 91-96 2014.

[29] P. Livieri, F. Berto, P. Lazzarin, Local strain energy approach applied to fatigue analysis of welded rectangular hollow section joints, International Journal of Materials & Product Technology, **30** 1-3 124-140, 2007.

[30] K. Golos, F. Ellyn, A Total Strain Energy Density Theory for Cumulative Fatigue Damage, Journal of Pressure Vessel, **110** 1 36-41, 2009.

[31] F. Berto, P. Lazzarin, Fatigue strength of Al7075 notched plates based on the local SED averaged over a control volume, SCIENCE CHINA, Physics, Mechanics & Astronomy, **57** 1 30-38, 2014

[32] P. Lazzarin, M. Zappalorto, F. Berto, Averaged strain energy density and J-integral for U- and blunt V-shaped notches under torsion, International Journal of Fracture, **188** 2 173-186, 2014.

[33] R. Afshar, F. Bero, P. Lazzarin, L.P. Pook, Analytical expressions for the notch stress intensity factors of periodic V-notches under tension by using the strain energy density approach, Journal of StrainA for Engineering Design, **48** 5 291-305, 2013.

[34] M. Zappalorto, P. Lazzarin, A Strain energy-based evaluations of plastic notch stress intensity factors at pointed V-notches under tensio, Engineering Frature Mechanics, **78** 15 2691-2706, 2011.

[35] A.R.. Torabi, M.R. Jafarinezhad, Comprehensive data for rapid calculation of notch stress intensity factors in U-notched Brazilian disc specimen under tensile-shear loading, Materials Science and Engineering A, 541 135-142, 2012.

[36] L. Bian, F. Taheri, Fatigue fracture criteria and microstructures of magnesium alloy plates, Materials Science and Engineering A, 487 1-2 74-85, 2008.

[37] K.O. Lee, S.G. Hong, S.B., Lee, A new energy-based fatigue damage parameter in life prediction of high-temperature structural materials, Materials Science and Engineering A, **496** 1-2 471-477, 2008.

[38] K.H. Bae, H.H. Kim, S.B. Lee, A simple life prediction method for 304L stainless steel structures under fatigue-dominated thermo-mechanical fatigue loadings, Materials Science and Engineering A, **529** 370-377, 2011.

[39] M. Noban, H. Jahed, S. Winkler, A. Ince, Fatigue characterization and modeling of 30CrNiMo8HH under multiaxial loading, Materials Science and Engineering A, **528** 6 2484-2494, 2011.

[40] M. Smaga, E. Walter, D. Eifler, Deformation-induced martensitic transformation in metastable austenitic steels, Materials Science and Engineering A, **483**-84 394-397, 2008.

[41] S.G. Hong, S.B. Lee, T.S., Byun, Temperature effect on the low-cycle fatigue behavior of type 316L stainless steel: Cyclic non-stabilization and an invariable fatigue parameter, Materials Science and Engineering A, **457** 1-2 1391-147, 2007.

[42] ASTM E739-91, Standard Practice for Statistical Analysis of Linear or Linearized Stress–life (S–N) and Strain–Life (E–N) Fatigue Data, ASTM International, 2004.

[43] A.K. Lakshminarayanan, V. Balasubramanian, Assessment of fatigue life and crack growth resistance of friction stir welded AISI 409M ferritic stainless steel joints. Materials Science and Eng. A, **539** 143–153, 2012.